NONLINEAR DELAY MONOPOLY WITH BOUNDED RATIONALITY

AKIO MATSUMOTO AND FERENC SZIDAROVSZKY

Abstract. The purpose of this paper is to study dynamics of a monopolistic firm in a continuous-time framework. The firm is assumed to be boundedly rational and to experience time delays in obtaining and implementing information on output. A dynamic adjustment process is based on the gradient of the expected profit. The paper is divided into three parts: We examine delay effects on dynamics caused by one-time delay and two-time delays in the first two parts. Global dynamics and analytical results on local dynamics are numerically confirmed in the third part. Four main results are demonstrated. First, the stability switch from stability to instability occurs only once in the case of the one-time delay. Second, the alternation of stability and instability can continue if two time delays are involved. Third, the birth of Hopf bifurcation is analytically shown if stability is lost. Finally, in a bifurcation process, there are a period-doubling cascade to chaos and a period-halving cascade to the equilibrium point in the case of two time delays if the difference between two the delays is large.

Keywords: single and multiple fixed time delays, Hopf bifurcation, bounded rationality, stability switch, nonlinear monopoly, gradient dynamics

JEL Classification: C62, C63, D42

The authors highly appreciate financial supports form the Japan Society for the Promotion of Science (Grant-in-Aid for Scientific Research (C) 21530172), Chuo University (Joint Research Grant 0981) and the Japan Economic Research Foundation. The research leading to this paper started when the first author visited the Department of Systems and Industrial Engineering of the University of Arizona and finished when the second author visited the Department of Economics, Chuo University. They appreciated hospitalities of those universities over their stay. The usual disclaimer applies.

1. Introduction

Traditional monopoly market has a structure in which there is only one seller, called a monopolistic firm, and there are infinitely many small buyers whose behavior is described by the market demand function. Further, the firm is assumed to be *rational* in a sense that full information or knowledge on demand is available to it without any delays. As a result, it is enough for the firm to select either price or quantity (but not both) to maximize profit. Once one of price and quantity is chosen, then the other is automatically determined through demand. No matter which choice is made, it can jump to the same optimum point in one shot without any dynamic considerations. Full information is, thus, the most important to make an optimal decision and to realize it. However, at the same time, it is very difficult, expensive and time-consuming to obtain. In reality, the monopolistic firm has only limited information. In addition to full information, most existing studies also assume the availability of instantaneous information. This may be due to mathematical convenience and is against actual observations that a seller usually obtains price information and sales data with some delays and reacts cautiously. Getting closer to the real world and making the monopoly theory more convincing, we replace this extreme assumption with the more plausible behavior assumption in which full and instantaneous information is eliminated. First, it is assumed that the monopolistic firm knows only a few points on the demand. A natural consequence of this alternation is that the firm is not able to move to the optimal point with one shot but gropes for it. Second, it is assumed that in revising the decisions, the firm experiences time delays inherent in phenomena like information and implementation delays. Such a firm is called *boundedly rational*. Therefore, we aim at studying a dynamic model of a boundedly rational monopolistic firm in order to describe an adjusting process of optimal decisions with time delays.

In constructing dynamic economic models, the most common processes are based on either the gradients of the profit functions or the best replies of the economic agents. Time delays can be modeled in two different ways: fixed time delays and continuously distributed time delays. The choice of "time", continuous time or discrete time, remains matter for debate. Cournot oligopoly is frequently discussed in a discrete-time model with the best replies. In the case of the gradient method, we mention the works of Bischi and Naimzada (1999) and Bischi and Lamantia (2002) for discrete-time oligopoly dynamics without time delays. Recent developments on the oligopoly theory can be found in Bischi *et al.* (2010) which contains models with both discrete and continuous time scales. Concerning discrete-time monopoly dynamics, we mention Puu (2003) and Naimzada (2011). The former assumes bounded rationality and shows that the monopolistic firm behaves in an erratic way. The latter exhibits that a fixed delay dynamics of the monopoly with bounded rationality can be described by the well-known logistic equation when the firm takes a learning activity of revising decisions.

In recent years it has been recognized in continuous-time economic dynamics that a delay differential equation is useful to describe the periodic and aperiodic behavior of economic variables. Howroyd and Russel (1984) detect the stability conditions of delay output adjustment processes in a general N-firm oligopoly with fixed time delays. On the other hand, Chiarella and Khomin (1996) and Chiarella and Szidarovszky (2001) examine delay differential oligopolies with best replies by using continuously distributed time delays. Furthermore, Bélair and Mackey

(1989) develop a model of price adjustment with production delays, Invernizzi and Medio (1991) investigate various economic models with continuously distributed delays and confirm analytically as well as numerically the conditions for chaotic solution. Recently, Matsumoto (2009) reconstructs Goodwin's accelerator model as a delay neutral differential equation and makes it clear that multiple limit cycles coexist whereas Matsumoto and Szidarovszky (2011a) introduce a fixed delay in production and a mound-shaped production function into the neoclassical one-sector growth model and show the birth of complex dynamics. With the infinite dimensionality created by a fixed-time delay, even a single first-order equation is transformed into an equation with a sufficient number of degrees of freedom to permit the occurrence of complex dynamics involving chaotic phenomena. This finding indicates that fixed-time delay models of a dynamic economy may explain various complex dynamic behavior of the economic variables. In addition to this, dynamics of a delay differential monopoly with the gradient method has not yet been revealed in the existing literature. Therefore, in this study, we draw our attention to dynamics of a continuous-time and fixed-delay monopoly under a circumstance where a firm is boundedly rational and uses the gradient of the expected profit to revise its output decision.

The paper is organized as follows. Section 2 constructs a basic monopoly model with linear price and cost functions and then introduces time delay; single time delay in the first part and multiple time delays in the second part. Local stability conditions are derived and the birth of a Hopf bifurcation is studied. Section 3 performs numerical simulations to confirm global behavior of a unstable monopoly equilibrium. Section 4 concludes the paper.

2. Delay Monopoly

Consider optimal behavior of a boundedly rational monopolistic firm which produces output q with marginal cost c. The price function is linear

$$f(q) = a - bq,\ a,\ b > 0.$$

We confine attention to a situation where the firm can estimate the derivative of the expected profit by using actual prices and demands it received in the past, although it does not know the price function and does not even know that it is linear. The estimated derivative at a value q^e of output is assumed to be

$$\frac{d\pi^e}{dq^e} = a - c - 2bq^e.$$

So the approximating gradient dynamics is

$$\dot{q} = \alpha(q)\frac{d\pi^e}{dq^e} \tag{2.1}$$

where $\alpha(q)$ is an adjustment function and the dot over a variable means a time derivative. In constructing best response dynamics, global information is required about the profit function, however, in applying gradient dynamics, only local information is needed. We make the familiar assumption that the adjustment function is linear in output:

Assumption 1.: $\alpha(q) = \alpha q$ with $\alpha > 0$.

The gradient dynamics under Assumption 1 with an expected output is presented by

$$\dot{q}(t) = \alpha q(t)\left[a - c - 2bq^e(t)\right] \tag{2.2}$$

where t denotes a point of continuous time.

2.1. **Single Fixed-Delay.** Dynamics depends on the formation of expectations. We start with a simple case in which at time t, the firm forms its expected demand to be equal to realized demand at time $t-\tau,\ \tau > 0$. Since it can be supposed that the actual output produced at time $t-\tau$ is equal to relaized demand at the same time, the expected demand is given in terms of output:

Assumption 2: $q^e(t) = q(t-\tau)$.

Replacing $q^e(t)$ in equation (2.2) with $q(t-\tau)$, we obtain the output adjustment process as a nonlinear differential equation with one fixed-time delay:

$$\dot{q}(t) = \alpha q(t)\left[a - c - 2bq(t-\tau)\right]. \tag{2.3}$$

Equation (2.3) has two stationary points; a trivial point $q(t) = 0$ and a nontrivial point

$$q^M = \frac{a-c}{2b}$$

where $a > c$ is assumed to ensure a positive stationary output. We may call q^M a monopoly equilibrium.

Our first concern is upon local stability of q^M. For this purpose, we analyze the linearized version of (2.3) about the monopoly equilibrium. Linearization and introduction of the new variable $x(t) = q(t) - q^M$ reduce equation (2.3) to

$$\dot{x}(t) = -\gamma x(t-\tau) \text{ with } \gamma = \alpha(a-c) > 0, \tag{2.4}$$

which has the zero-solution, $x(t) = 0$ (or $q(t) = q^M$) for all $t \geq 0$. If there is no time delay, $\tau = 0$, then equation (2.4) becomes an ordinary differential equation and has a stable solution, $x_0 e^{-\gamma t}$, where x_0 is an initial point. If there is a positive time delay, $\tau > 0$, then equation (2.4) becomes a linear delay differential equation where initial data are given by a continuous function defined for $-\tau \leq t \leq 0$. It is impossible to derive an explicit solution even though the equation seems to be simple. In spite of this inconvenience, it is possible to analyze qualitative aspects of the solution in the following way. Substituting the exponential solution $x(t) = x_0 e^{\lambda t}$ into (2.4) yields the following characteristic equation associated with the linearized delay equation:

$$\lambda + \gamma e^{-\lambda\tau} = 0. \tag{2.5}$$

The sufficient condition for local asymptotical stability of the zero-solution is that the real parts of the eigenvalues are negative.

The characteristic equation is a function of τ and so are its roots. It is seen that the zero solution is asymptotically stable for $\tau = 0$. By continuity we expect that it remains asymptotically stable with small values of τ. Equation (2.5) implies that the real roots are at the intersection of an exponential curve (i.e., $e^{-\lambda\tau}$) and a negative-sloping straight line (i.e., $-\lambda/\gamma$). We have two real roots, one real root or no real root, depending on the value of τ. It can be shown that the line is tangent to the curve at $\tau\gamma = 1/e$. For τ satisfying the tangency condition, equation (2.5) generates a unique negative root. Further increases of τ, *ceteris paribus*, may change the zero real part of λ to positive making the system unstable. Such phenomena is

referred to as a *stability switch.* In order to understand the stability switch of (2.4), it is crucial to determine a threshold value $\tau = \tau^*$ at which the real parts of the complex roots of (2.5) are zero and their derivatives are positive. We then assume, without loss of generality, that $\lambda = i\upsilon$, $\upsilon > 0$, is a root of (2.5) for $\tau = \tau^*$. In order to hold equation (2.5) under $\upsilon > 0$, the real and imaginary parts must satisfy the followings:

$$\gamma \cos \upsilon\tau = 0$$

and

$$\upsilon - \gamma \sin \upsilon\tau = 0.$$

Adding up the squares of both equations yields $\upsilon^2 = \gamma^2$ from which we obtain

$$\upsilon = \gamma.$$

The necessary and sufficient conditions for the existence of a pair of purely imaginary roots are

$$\cos \upsilon\tau = 0$$

and

$$\sin \upsilon\tau = \frac{\upsilon}{\gamma} = 1$$

from which we have infinitely many solutions,

$$\tau = \frac{1}{\gamma}\left(\frac{\pi}{2} + 2n\pi\right), \ n = 0, 1, 2, ... \tag{2.6}$$

The real parts of the roots are zero for τ satisfying (2.6). We now detect the stability switch at which the equilibrium loses stability. Since λ is a function of delay τ, we need the minimum solution of τ for which a derivative of $\lambda(\tau)$ is positive. By selecting τ as the bifurcation parameter and differentiating the characteristic equation (2.5) with respect to τ yield

$$(1 - \gamma\tau e^{-\lambda\tau})\frac{d\lambda}{d\tau} = \gamma\lambda e^{-\lambda\tau}.$$

which is reduced to

$$\left(\frac{d\lambda}{d\tau}\right)^{-1} = \frac{1 - \gamma\tau e^{-\lambda\tau}}{\gamma\lambda e^{-\lambda\tau}}.$$

Obtaining $e^{-\lambda\tau} = -\lambda/\gamma$ from (2.5) and substituting it into the last equation, we can show that the real parts are positively sensitive to a change in τ,

$$\mathrm{Re}\left[\left(\frac{d\lambda}{d\tau}\right)^{-1}\Bigg|_{\lambda=i\nu}\right] = \frac{1}{\upsilon^2} > 0 \text{ or } \left.\frac{d(\mathrm{Re}\,\lambda)}{d\tau}\right|_{\lambda=i\nu} > 0.$$

This inequality implies that all roots that cross the imaginary axis at $i\upsilon$ cross from left to right as τ increases. Matsumoto and Szidarovszky (2011b) demonstrate that stability switch does not occur for any $\tau > \pi/(2\gamma)$ given in (2.6), although the real parts are zero and their derivatives with respect to τ are non-zero. Hence the threshold value of τ is

$$\tau^* = \frac{\pi}{2\gamma}$$

This result is summarized as follows:

Theorem 1. *The delay output adjustment process (2.3) has a threshold value τ^* of delay: The monopoly equilibrium is locally asymptotically stable for $0 < \tau < \tau^*$, locally unstable for $\tau > \tau^*$ and undergoes a Hopf bifurcation at $\tau = \tau^*$ where τ^* is defined by*

$$\tau^* = \frac{\pi}{2\alpha(a-c)}.$$

Theorem 1 is visualized in Figure 1(A) where the higher hyperbolic downward sloping curve is the locus of $\tau\gamma = \pi/2$ and the lower hyperbolic curve is the locus of $\pi\gamma = 1/e$. The latter curve is a partition curve between the real roots and the complex roots. The former curve is the stability switch curve that divides the first quadrant of the the (γ, τ) plane into two regions: the gray region in which the monopoly equilibrium is locally stable and the white region in which it is locally unstable. Although local stability (instability) implies global stability (instability) in a linear model, this is not necessarily a case in nonlinear dynamic system such as (2.3)[1]. To observe global behavior of the unstable equilibrium, we perform numerical simulations. Taking $\alpha = 1/2$, $a = 3$, $c = 1$, $b = 1$ and $\gamma = 1$, we select four parametric combinations of (γ, τ) indicated by the black points along the vertical line at $\gamma = 1$ in the white region of Figure 1(A). Corresponding dynamics are described by limit cycles with different amplitudes as shown in Figure 1(B). It can be seen that the amplitude becomes larger as the delay becomes longer.

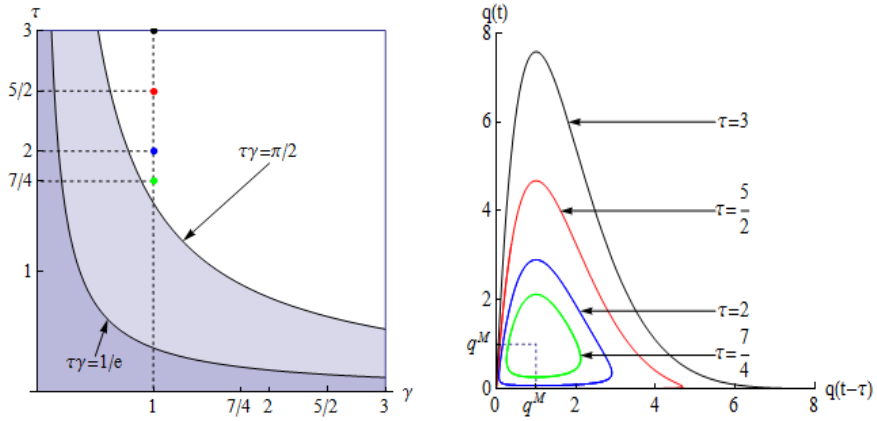

(A) Divisions of the (γ, τ) plane (B) Birth of limit cycles

Figure 1. Dynamics with one delay

2.2. **Multiple Fixed-Delays.** We next examine stability of the monopoly equilibrium when the estimate of the price function is based on a weighted average of past estimates at two different times, $t - \tau_1 > 0$ and $t - \tau_2 > 0$, which is the same as estimating the derivative of the price function with a linear combination of two

[1]Using a logistic single species population model, which is essentially the same as the delay monopoly model (2.3), Wright (1955) shows global stability under the condition of $\tau < 3/2\gamma$ and presumes that his method can be used to extend the global result to $\tau < 2\pi/\gamma$. However this conjecture still remains open.

past output values. Similarly to the case of a single fixed delay we have now the following assumption:

Assumption 3: $q^e(t) = \omega q(t-\tau_1) + (1-\omega)q(t-\tau_2)$ with $0 < \omega < 1$.

Replacing $q^e(t)$ in equation (2.2) with this weighted average, we obtain the output adjustment process as a differential equation with two fixed-time delays,

$$\dot{q}(t) = \alpha q(t)\left[a - c - 2b\left(\omega q(t-\tau_1) + (1-\omega)q(t-\tau_2)\right)\right]. \tag{2.7}$$

Notice that q^M is also a positive stationary state of (2.7). As in the single delay case, we first analyze local stability of q^M. Linearizing equation (2.7) in a neighborhood of the stationary point and using $x(t) = q(t) - q^M$ yield a linear delay equation,

$$\dot{x}(t) = -\gamma[\omega x(t-\tau_1) + (1-\omega)x(t-\tau_2)]. \tag{2.8}$$

Looking for a solution $x(t) = x_0 e^{\lambda t}$ presents the characteristic equation

$$\lambda + \gamma\omega e^{-\lambda\tau_1} + \gamma(1-\omega)e^{-\lambda\tau_2} = 0.$$

For notational simplicity, let

$$\bar{\lambda} = \frac{\lambda}{\gamma},\ \gamma_1 = \gamma\tau_1 \text{ and } \gamma_2 = \gamma\tau_2$$

which lead to the simplified form,

$$\bar{\lambda} + \omega e^{-\bar{\lambda}\gamma_1} + (1-\omega)e^{-\bar{\lambda}\gamma_2} = 0.$$

Dropping the bar from $\bar{\lambda}$, we obtain the normalized characteristic equation,[2]

$$\lambda + \omega e^{-\lambda\gamma_1} + (1-\omega)e^{-\lambda\gamma_2} = 0. \tag{2.9}$$

When $\gamma_1 = \gamma_2$, equation (2.9) is reduced to equation (2.5). Thus $\gamma_1 \neq \gamma_2$ is assumed henceforth. Three cases are identified: (1) $\omega > 1/2$, (2) $\omega = 1/2$ and (3) $\omega < 1/2$. Since the first and third cases are symmetric, we confine attention to the case of $\omega \geq 1/2$.

We construct the loci of (γ_1, γ_2) on which the real part of an eigenvalue is zero. We thus assume that $\lambda = iv$ with $v > 0$ is a root of equation (2.9) satisfying

$$iv + \omega e^{-iv\gamma_1} + (1-\omega)e^{-iv\gamma_2} = 0. \tag{2.10}$$

Real and imaginary parts are

$$\omega\cos(v\gamma_1) + (1-\omega)\cos(v\gamma_2) = 0 \tag{2.11}$$

and

$$v - \omega\sin(v\gamma_1) - (1-\omega)\sin(v\gamma_2) = 0. \tag{2.12}$$

---

[2]Suppose that the characteristic equation is

$$\lambda + \gamma A e^{-\lambda\tau_1} + \gamma B e^{-\lambda\tau_2} = 0$$

where the weights A and B are positive constants and $A + B \neq 1$. Dividing it by $\gamma(A+B)$ yields

$$\frac{\lambda}{\gamma(A+B)} + \gamma\frac{A}{\gamma(A+B)}e^{-\lambda\tau_1} + \gamma\frac{B}{\gamma(A+B)}e^{-\lambda\tau_2} = 0.$$

Let

$$\bar{\lambda} = \frac{\lambda}{\gamma(A+B)},\ \gamma_i = (A+B)\gamma\tau_i,\ \omega = \frac{A}{A+B},$$

then the resultant characteristic equation has essentially the same form as the one in (2.9).

When the real part of an eigenvalue changes sign, then the corresponding point (γ_1, γ_2) has to be on the loci satisfying (2.11) and (2.12). Then we call it a stability-switch curve. As derived in Appendix I, it consists of the two segments, one segment is denoted by $L_1(k,n)$ and the other by $L_2(k,n)$ for each $k, n \in \mathbb{N}$:

$$L_1(k,n): \begin{cases} \gamma_1 = \dfrac{1}{\upsilon}\left(\sin^{-1}\left[\dfrac{\upsilon^2+2\omega-1}{2\upsilon\omega}\right] + 2k\pi\right) \\ \gamma_2 = \dfrac{1}{\upsilon}\left(\pi - \sin^{-1}\left[\dfrac{\upsilon^2-2\omega+1}{2\upsilon(1-\omega)}\right] + 2n\pi\right) \end{cases} \tag{2.13}$$

and

$$L_2(k,n): \begin{cases} \gamma_1 = \dfrac{1}{\upsilon}\left(\pi - \sin^{-1}\left[\dfrac{\upsilon^2+2\omega-1}{2\upsilon\omega}\right] + 2k\pi\right) \\ \gamma_2 = \dfrac{1}{\upsilon}\left(\sin^{-1}\left[\dfrac{\upsilon^2-2\omega+1}{2\upsilon(1-\omega)}\right] + 2n\pi\right) \end{cases} \tag{2.14}$$

Specifying the value of ω, we examine the shapes of $L_1(k,n)$ and $L_2(k,n)$.

Asymmetric weights: $\omega > \frac{1}{2}$:

Using equations (2.13) and (2.14), we can compute the starting point (γ_1^s, γ_2^s) and the end point (γ_1^e, γ_2^e) of $L_1(k,n)$:

$$\gamma_1^s = \frac{1}{2\omega-1}\left(\frac{\pi}{2} + 2k\pi\right) \text{ and } \gamma_2^s = \frac{1}{2\omega-1}\left(\frac{3\pi}{2} + 2n\pi\right),$$

$$\gamma_1^e = \frac{\pi}{2} + 2k\pi \text{ and } \gamma_2^e = \frac{\pi}{2} + 2n\pi,$$

and the starting point (γ_1^S, γ_2^S) and the end point (γ_1^E, γ_2^E) of $L_2(k,n)$ are

$$\gamma_1^S = \frac{1}{2\omega-1}\left(\frac{\pi}{2} + 2k\pi\right) \text{ and } \gamma_2^S = \frac{1}{2\omega-1}\left(-\frac{\pi}{2} + 2n\pi\right),$$

$$\gamma_1^E = \frac{\pi}{2} + 2k\pi \text{ and } \gamma_2^E = \frac{\pi}{2} + 2n\pi.$$

Notice that γ_2^S is infeasible at $n = 0$. Since $\gamma_2 = 0$ for $\upsilon = \sqrt{2\omega-1}$, only the segment of $L_2(0,0)$ between $\sqrt{2\omega-1}$ and 1 is feasible. Notice also that $(\gamma_1^e, \gamma_2^e) = (\gamma_1^E, \gamma_2^E)$ and $(\gamma_1^s, \gamma_2^s) = (\gamma_1^S, \gamma_2^S + 2\pi/(2\omega-1))$ with fixed k. The first equality implies that $L_1(k,n)$ and $L_2(k,n)$ have the same end point while the second equality indicates that the starting point of $L_1(k,n)$ is the same as that of $L_2(k,n+1)$. Therefore the $L_1(k,n)$ and $L_2(k,n)$ segments form a continuous curve with $n = 0, 1, 2...$ It can be confirmed that both segments shift upward as n increases with given k and rightward as k increases with given n. We summarize these properties of $L_1(k,n)$ and $L_2(k,n)$ as follows:

Proposition 1. *(1) Given k and n, the end point of $L_1(k,n)$ is the same as the end point of $L_2(k,n)$ while the starting point of $L_1(k,n)$ is the same as the starting point of $L_2(k,n+1)$. (2) The loci shift upward if n increases and k is fixed whereas it shifts rightward if k increases and n is fixed.*

The monotonicity of the loci, $L_1(k,n)$ and $L_2(k,n)$, as well as their extreme (minimum and maximum) values can be examined based on the derivatives $\partial\gamma_1/\partial\upsilon$ and $\partial\gamma_2/\partial\upsilon$, which are presented in Appendix II. It is derived there that for $j = 1, 2$,

$$sign\left[\left.\frac{\partial\gamma_1}{\partial\upsilon}\right|_{L_j(k,n)}\right] = -sign\left[\upsilon\gamma_1 + \tan(\upsilon\gamma_2)\right]$$

and

$$sign\left[\left.\frac{\partial\gamma_2}{\partial\upsilon}\right|_{L_j(k,n)}\right] = -sign\left[\upsilon\gamma_2 + \tan(\upsilon\gamma_1)\right]$$

In order to simplify further discussions we change the coordinates (γ_1, γ_2) to $(\upsilon\gamma_1, \upsilon\gamma_2)$ to get the transformed segments:

$$\ell_1(k,n): \begin{cases} \upsilon\gamma_1 = \sin^{-1}\left[\dfrac{\upsilon^2 + 2\omega - 1}{2\upsilon\omega}\right] + 2k\pi \\ \\ \upsilon\gamma_2 = \pi - \sin^{-1}\left[\dfrac{\upsilon^2 - 2\omega + 1}{2\upsilon(1-\omega)}\right] + 2n\pi \end{cases}$$

and

$$\ell_2(k,n): \begin{cases} \upsilon\gamma_1 = \pi - \sin^{-1}\left[\dfrac{\upsilon^2 + 2\omega - 1}{2\upsilon\omega}\right] + 2k\pi \\ \\ \upsilon\gamma_2 = \sin^{-1}\left[\dfrac{\upsilon^2 - 2\omega + 1}{2\upsilon(1-\omega)}\right] + 2n\pi \end{cases}$$

They also form continuous curves with fixed k for $n = 0, 1, 2, ...$, which are periodic in both directions $\upsilon\gamma_1$ and $\upsilon\gamma_2$. Figure 2(A) shows these segments with $k = 0$ and $n = 0, 1$.

In order to see the monotonicity of the loci we also show the curves

$$\upsilon\gamma_1 = -\tan(\upsilon\gamma_2) \text{ and } \upsilon\gamma_2 = -\tan(\upsilon\gamma_1)$$

in Figure 2(A) where the former defined for the three domains of $\upsilon\gamma_2$, $(\pi/2, 3\pi/2)$, $(3\pi/2, 5\pi/2)$ and $(5\pi/2, 7\pi/2)$ is illustrated by the flatter real curves and the latter defined for $\upsilon\gamma_1 \in (\pi/2, \pi)$ is by the steeper curve. Let us see the monotonicity of $L_1(0,0)$ first. Locus $\ell_1(0,0)$ has an intercept denoted as m_0 with the curve $\upsilon\gamma_1 = -\tan(\upsilon\gamma_2)$ for $\upsilon\gamma_2 \in (\pi/2, 3\pi/2)$. Before this intercept (in the direction of increasing value of υ which is indicated by the arrows) γ_1 decreases in υ, after the intercept, increases. Therefore this point corresponds to the minimum value of γ_1 on $L_1(k,n)$, denoted by γ_1^m in Figure 2(B). On $\ell_1(k,n)$, $\upsilon\gamma_2 > -\tan(\upsilon\gamma_1)$ everywhere, so γ_2 decreases in υ here. Consequently, the slope of $L_1(0,0)$ defined by

$$\frac{\partial\gamma_2}{\partial\gamma_1} = \frac{\partial\gamma_2/\partial\upsilon}{\partial\gamma_1/\partial\upsilon}$$

is positive along the corresponding part from S_0 to m_0 of $L_1(0,0)$ and the inequality is reversed along the remaining part from m_0 to E_0 as shown in Figure 2(B). We now turn attention to the monotonicity of the $L_2(0,0)$ curve. Locus $\ell_2(0,0)$ has an intercept with the curve $\upsilon\gamma_1 = -\tan(\upsilon\gamma_2)$ for $\upsilon\gamma_2 \in (-\pi/2, \pi/2)$. Since its ordinate is negative, the intercept is not shown in Figure 2(A). It is checked that $\partial\gamma_1/\partial\upsilon < 0$ and $\partial\gamma_2/\partial\upsilon > 0$, which then imply $\partial\gamma_2/\partial\gamma_1 < 0$ along the $L_2(0,0)$ locus.

The starting point S_0 and end point E_1 of the $L_2(0,1)$ locus are given by

$$\left(\frac{\pi}{2(2\omega-1)}, \frac{3\pi}{2(2\omega-1)}\right) \text{ and } \left(\frac{\pi}{2}, \frac{5\pi}{2}\right)$$

where the ordinates of these points are the same

$$\frac{3\pi}{2(2\omega-1)} = \frac{5\pi}{2} \text{ if } \omega = 0.8.$$

Since the $\ell_2(0,1)$ locus intercepts once with the $\upsilon\gamma_1 = -\tan(\upsilon\gamma_2)$ curve at point M and twice with the $\upsilon\gamma_2 = -\tan(\upsilon\gamma_1)$ curve at points A and B, the corresponding curve of $L_2(0,1)$ takes non-monotonic shape. Let see this more precisely. As υ increases from $2\omega-1$ to 1, the point $(\upsilon\gamma_1, \upsilon\gamma_2)$ moves along the $\ell_2(0,1)$ locus from S_0 to E_1. Before intercept M, $\upsilon\gamma_1 < -\tan(\upsilon\gamma_2)$ showing that γ_1 increases in υ, and after this intercept, γ_1 decreases, so this point corresponds to the maximum value of γ_1 on $L_2(k,n)$, denoted by γ_1^M. Since we have $\upsilon\gamma_2 < -\tan(\upsilon\gamma_1)$ in the left of the $\upsilon\gamma_2 = -\tan(\upsilon\gamma_1)$ curve and $\upsilon\gamma_2 > -\tan(\upsilon\gamma_1)$ in the right, γ_2 decreases between the two intercepts A and B, and increases otherwise. Therefore the first intercept corresponds to the maximum value of γ_2 and the second corresponds to the minimum value of γ_2 on $L_2(k,n)$. By the three intersections between S_0 and E_1, the whole $L_2(0,1)$ locus is divided into four pieces, along each of which we have the following slopes in the (γ_1, γ_2) plane,

$$\begin{aligned}
&(1)\ \frac{\partial\gamma_2}{\partial\gamma_1} > 0 \text{ as } \frac{\partial\gamma_1}{\partial\upsilon} > 0 \text{ and } \frac{\partial\gamma_2}{\partial\upsilon} > 0 \text{ between } S_0 \text{ and } M,\\
&(2)\ \frac{\partial\gamma_2}{\partial\gamma_1} < 0 \text{ as } \frac{\partial\gamma_1}{\partial\upsilon} < 0 \text{ and } \frac{\partial\gamma_2}{\partial\upsilon} > 0 \text{ between } M \text{ and } A,\\
&(3)\ \frac{\partial\gamma_2}{\partial\gamma_1} > 0 \text{ as } \frac{\partial\gamma_1}{\partial\upsilon} < 0 \text{ and } \frac{\partial\gamma_2}{\partial\upsilon} < 0 \text{ between } A \text{ and } B,\\
&(4)\ \frac{\partial\gamma_2}{\partial\gamma_1} < 0 \text{ as } \frac{\partial\gamma_1}{\partial\upsilon} < 0 \text{ and } \frac{\partial\gamma_2}{\partial\upsilon} > 0 \text{ between } B \text{ and } E_1.
\end{aligned}$$

In the same way, we can depict the loci of $L_1(k,n)$ and $L_2(k,n)$ for any other values of k and n. Notice that all the segments of $L_1(k,n)$ and $L_2(k,n)$ are located within the interval $[\gamma_1^m, \gamma_1^M]$. In Figure 2(B) with the parameter values specified above,

$$\gamma_1^m \simeq 1.493 \text{ and } \gamma_1^M \simeq 2.733.$$

In Figure 2(A), the maximum and minimum values of $\upsilon\gamma_1$ on $\ell_i(k,n)$ are given by

$$\upsilon^m\gamma_1^m \simeq 1.427 \text{ and } \upsilon^M\gamma_1^M \simeq 1.715$$

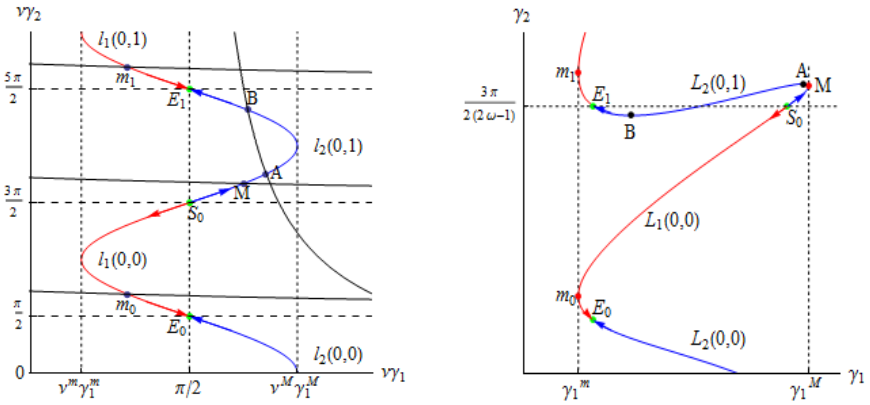

(A) In the $(\upsilon\gamma_1, \upsilon\gamma_2)$ plane (B) In the (γ_1, γ_2) plane

Figure 2. Partition curves

We now turn our attention to the stability of the monopoly equilibrium. Needless to say, q^M is asymptotically locally stable when $\tau_1 = \tau_2 = 0$. By continuity, it is locally asymptotically stable if τ_1 and τ_2 are sufficiently small. Since the segments of $L_1(k,n)$ and $L_2(k,n)$ are located within the interval $[\gamma_1^m, \gamma_1^M]$, the vertical line with $\gamma_1 < \gamma_1^m$ crosses none of these segments. Therefore the output adjustment process is asymptotically stable regardless of the values of $\gamma_2 > 0$ if γ_1 is strictly less than γ_1^m. Such delays of (γ_1, γ_2) are called *harmless* and belong to the light-gray rectangle in the left of Figure 3.

Next we investigate stability for $\gamma_1 > \gamma_1^m$ and the occurrence of Hopf bifurcation. Fixing $\gamma_2 > 0$, we choose γ_1 as a bifurcation parameter and then differentiate the characteristic equation (2.9) having $\lambda = \lambda(\gamma_1)$ with respect to γ_1 to obtain

$$\frac{d\lambda}{d\gamma_1} + \omega e^{-\lambda\gamma_1}\left(-\frac{d\lambda}{d\gamma_1}\gamma_1 - \lambda\right) + (1-\omega)e^{-\lambda\gamma_2}\left(-\frac{d\lambda}{d\gamma_1}\gamma_2\right) = 0.$$

Solving this for the inverse of $d\lambda/d\gamma_1$ gives

$$\begin{aligned}\left(\frac{d\lambda}{d\gamma_1}\right)^{-1} &= \frac{1-\omega\gamma_1 e^{-\lambda\gamma_1} - (1-\omega)\gamma_2 e^{-\lambda\gamma_2}}{\lambda\omega e^{-\lambda\gamma_1}} \\ &= \frac{1-\omega\gamma_1 e^{-\lambda\gamma_1} + \gamma_2(\lambda + \omega e^{-\lambda\gamma_1})}{\lambda\omega e^{-\lambda\gamma_1}} \\ &= \frac{1+\lambda\gamma_2}{\lambda\omega e^{-\lambda\gamma_1}} + \frac{\omega(\gamma_2-\gamma_1)}{\lambda\omega}\end{aligned}$$

where we used the characteristic equation (2.9). If $\lambda = i\upsilon$, then

$$\begin{aligned}\mathrm{Re}\left(\frac{d\lambda}{d\gamma_1}\right)^{-1} &= \mathrm{Re}\,\frac{1+i\upsilon\gamma_2}{i\upsilon\omega(\cos(\upsilon\gamma_1) - i\sin(\upsilon\gamma_1))} \\ &= \frac{\sin(\upsilon\gamma_1) + \upsilon\gamma_2\cos(\upsilon\gamma_1)}{\upsilon\omega}\end{aligned}$$

so $\mathrm{Re}(d\lambda/d\gamma_1)$ has the same sign as $\sin(\upsilon\gamma_1) + \upsilon\gamma_2\cos(\upsilon\gamma_1)$. With any fixed positive value of γ_2 we can gradually increase the value of γ_1 from zero until it intercepts with a segment $L_1(0,n)$ or $L_2(0,n)$. It is easy to prove that at this and each later intercepts there is a unique pure complex eigenvalue.

Assume first that γ_1 crosses a segment $L_1(0,n)$ from the left. There $\upsilon\gamma_1 \in (0,\pi/2)$ implying that both $\sin(\upsilon\gamma_1)$ and $\cos(\upsilon\gamma_1)$ are positive as well as $\mathrm{Re}(d\lambda/d\gamma_1) > 0$. Therefore stability is lost everywhere on the segments $L_1(0,n)$. Assume next that γ_1 crosses a segment $L_2(0,n)$ from the left where $\cos(\upsilon\gamma_1) \le 0$ as $\upsilon\gamma_1 \in [\pi/2,\pi]$. Stability is lost when $\mathrm{Re}(d\lambda/d\gamma_1) > 0$ at the intercept and the real part of an eigenvalue changes sign from positive to negative if $\mathrm{Re}(d\lambda/d\gamma_1) < 0$. If there was only one stability switch from negative to positive real part before, then stability is regained, since at the intercept with $L_2(0,n)$ the real part of the same eigenvalue changes back to negative. If there are more than one stability switches from negative to positive real parts before, then stability cannot be regained, since at least one eigenvalue will still have positive real part. Based on (4.13), it is clear that

$$\mathrm{Re}\left[\left.\frac{d\lambda}{d\gamma_1}\right|_{\lambda=i\upsilon}\right] = -\frac{\upsilon\cos(\upsilon\gamma_1)}{\omega}\left.\frac{\partial\gamma_2}{\partial\upsilon}\right|_{L_2(k,n)},$$

therefore $\mathrm{Re}(d\lambda/d\gamma_1) > 0$ when γ_2 increases in υ and $\mathrm{Re}(d\lambda/d\gamma_1) < 0$ when γ_2 decreases in υ. Hence stability is switched to instability when $\partial\gamma_2/\partial\upsilon > 0$ whereas instability might be switched to stability when $\partial\gamma_2/\partial\upsilon < 0$. Figure 3 illustrates these segments of $L_i(k,n)$ for $i = 1,2$ with the parameter values of $\alpha = 0.5,\ a = 3,\ b = c = 1,\ \omega = 0.8,\ k = 0$ and $n = 0,1,2$ when υ increases from $2\omega - 1$ to 1.[3] The points of $L_1(0,n)$ form the red curves, and those of $L_2(0,n)$ the blue curves while the green dotted points denoted as S_i and E_i are the starting and end points of $L_1(k,n)$ and $L_2(k,n)$ as indicated by the directions of the arrows.

When the real part of an eigenvalue changes from negative to positive, then stability is lost for sure. If the change is from positive to negative, then stability may be regained but not necessarily, as it is illustrated in the following two cases. If $\gamma_2 = \gamma_2^{(1)}$ as shown in Figure 3, then the first intercept is with $L_1(0,2)$ where stability is lost, since the real part of an eigenvalue becomes positive. If γ_1 is increased further, then there is a second intercept with $L_2(0,2)$ where the real part of the same eigenvalue becomes negative again, so stability is regained. If γ_1 is increased even further, then there is a third intercept with $L_1(0,1)$ where stability is lost again. However if we select $\gamma_2 = \gamma_2^{(2)}$, then we also have three intercepts, the first two are with $L_1(0,2)$ and $L_1(0,1)$, so two eigenvalues will have positive real parts, and the sign of only one of them changes back to negative at the third intercept with $L_2(0,2)$. Therefore in this case no stability switch occurs since stability cannot be regained. The stability region is the union of the light-gray and dark-gray areas. Hopf bifurcation occurs on the boundary curve between the gray region and the white region except where γ_2 is minimal or maximal on $L_2(0,n)$, which are not really crossing points.

If the value of γ_1 is fixed and γ_2 is the bifurcation parameter, then by using the same approach, the same stability region is derived and Hopf bifurcation occurs at the crossing points except if $\gamma_1 = \gamma_1^m$ or $\gamma_1 = \gamma_1^M$. These points are not crossing points, since the corresponding vertical line is the tangent line to $L_1(0,n)$ or $L_2(0,n)$. This is the same result which was obtained earlier by Hale and Huang (1993) and Matsumoto and Szidarovszky (2011c) and summarized as follows:

[3]We will soon refer to the two black dots denoted by A and B.

Theorem 2. *(1) Delays are harmless if* $\gamma_1 \leq \gamma_1^m$ *and* $\gamma_2 \geq 0$. *(2)* $L_1(0,n)$ *and* $L_2(0,n)$ *constitute a stability-switch curve; The monopoly equilibrium is locally asymptotically stable in the dark-gray region of Figure 3 and it is locally unstable in the white region.*

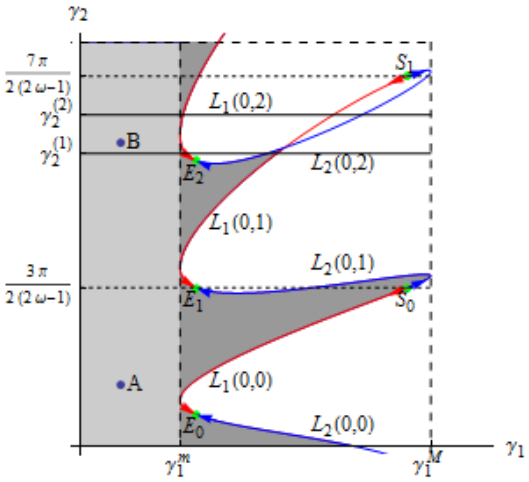

Figure 3. Stability-switch curve in the (γ_1, γ_2) plane with $k = 0$

Symmetric Weights: $\omega = \dfrac{1}{2}$**:**

Substituting $\omega = 1/2$ into (2.13) and (2.14) we obtain the loci with symmetric weights,[4]

$$L_1(k,n): \begin{cases} \gamma_1 = \dfrac{1}{\upsilon}\left(\sin^{-1}[\upsilon] + 2k\pi\right) \\ \gamma_2 = \dfrac{1}{\upsilon}\left(\pi - \sin^{-1}[\upsilon] + 2n\pi\right) \end{cases} \tag{2.15}$$

and

$$L_2(k,n): \begin{cases} \gamma_1 = \dfrac{1}{\upsilon}\left(\pi - \sin^{-1}[\upsilon] + 2k\pi\right) \\ \gamma_2 = \dfrac{1}{\upsilon}\left(\sin^{-1}[\upsilon] + 2n\pi\right). \end{cases} \tag{2.16}$$

Clearly υ has to be in the unit interval in order to have feasible solution.

Loci $L_1(k,n)$ and $L_2(k,n)$ for $k = 0, 1$ and $n = 0, 1$ are depicted as the red curves and the blue curves in Figure 4. When $k = n = 0$, these two loci construct a hyperbolic curve passing through the point $(\pi/2, \pi/2)$ which is the common end point of $L_1(0,0)$ and $L_2(0,0)$. The curve divides the (γ_1, γ_2) plane into two regions, a stable gray region in which all roots of the characteristic equation have strictly negative real part for (γ_1, γ_2) and a unstable white region in which the monopoly equilibrium becomes locally unstable, which can be proved similarly to the non-symmetric case. Notice that the curve is symmetric with respect to the diagonal

[4]Hale (1979) determines the geometry of the stability region with $\omega = 1/2$ in a different way.

and asymptotic to the lines $\gamma_i = 1$, since $\sin^{-1}(\upsilon)/\upsilon$ converges to 1 as $\upsilon \longrightarrow 0$. This implies that the monopoly equilibrium is locally asymptotically stable for any $\gamma_i > 0$ if $\gamma_j \leq 1$ for $i, j = 1, 2$ and $i \neq j$, in other word, the delays are harmless. We have the similar results as Proposition 2 in the case of $\omega = 1/2$:

Proposition 2. *(1) Given k and n, $L_1(k, n)$ and $L_2(k, n)$ defined on the unit interval $[0, 1]$ have the same end point. (2) Fixing k and increasing n shift the loci upward, while fixing n and increasing k shift the loci rightward. (3) Increasing k and n together shifts the loci along the diagonal line, $\gamma_1 = \gamma_2$.*

Stability results in the symmetric case are summarized as follows:

Theorem 3. *(1) Delays are harmless if $\gamma_i > 0$ and $\gamma_j \leq 1$ for $i, j = 1, 2$ and $i \neq j$. (2) $L_1(0, 0)$ and $L_2(0, 0)$ constitute a stability-switch curve, below which the monopoly equilibrium is locally asymptotically stable and above which it is locally unstable.*

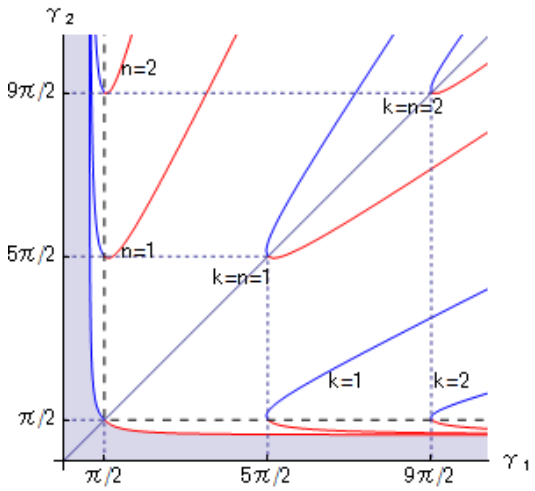

Figure 4. Divisions of the (γ_1, γ_2) plane when $\omega = \dfrac{1}{2}$

3. Numerical Simulations

In this section we perform simulations, first, to confirm the analytical results obtained above and, second, to see how the two delays affect global dynamic behavior. Throughout this section we take $\alpha = 0.5$, $a = 3$, $b = c = 1$ under which $\gamma = 1$ always implying $\gamma_i = \tau_i$ for $i = 1, 2$.

Harmless delays:

We examine harmless delays of γ_1 and γ_2 such that $\gamma_i \geq 0$ and $\gamma_j \leq \gamma_j^m$ for $i, j = 1, 2$ and $i \neq j$. Two combinations of (γ_1, γ_2) are selected from this region. Figure 5(A) illustrates a time trajectory of $q(t)$ for $\gamma_1 = 1.2$ and $\gamma_2 = 3$ which are ordinates at point A in Figure 3 and so does Figure 5(B) for $\gamma_1 = 1.2$ and $\gamma_2 = 15$,

which are ordinates of point B. Both trajectories take the same initial function, $\phi(t) = 0.1$ for $t \leq 0$, exhibit initial disturbances, which are sooner or later disappear and finally converge to the monopoly equilibrium. The initial disturbance with the larger delay of γ_2 is larger and more aperiodic than the one with the smaller delay of γ_2. The numerical simulations confirm the analytical result that delay γ_2 has no effect on asymptotic behavior of output if $\gamma_1 \leq \gamma_1^m$.

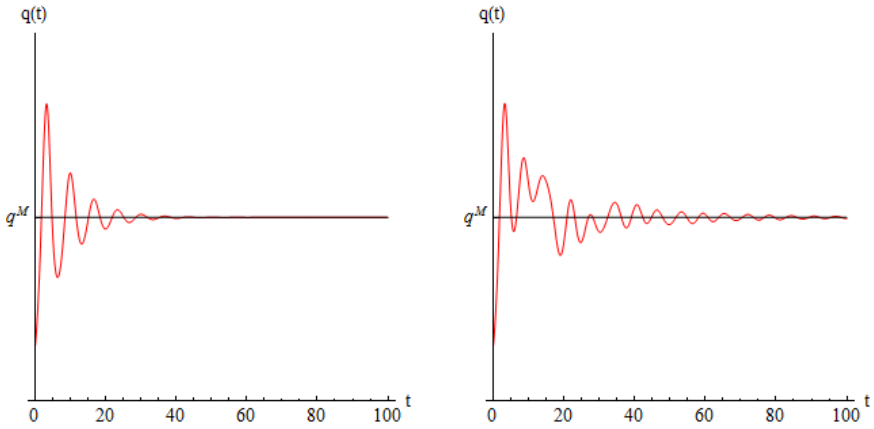

(A) $\gamma_1 = 1.2$ and $\gamma_2 = 3$ (B) $\gamma_1 = 1.2$ and $\gamma_2 = 15$

Figure 5. Convergnet trajectories when the delays are harmless

Bifurcation diagram:

To examine global behavior of the unstable equilibrium, we fix the value of γ_1 and increase γ_2 from 0 to $7\pi/(2(2w-1))$, the upper bound of γ_2 in Figure 3. For each value of τ_2, the delay equation (2.7) is solved to get a time series of $q(t)$, $q(t-\gamma_1)$ and $q(t-\gamma_2)$ for $1000 \leq t \leq 2000$. The extreme values (i.e., local maxima and local minima) of the time series $q(t)$ are plotted against γ_2. The resultant extremum-against-delay plot is called a bifurcation diagram with respect to γ_2 in a continuous time dynamical system.

Example 1: $\gamma_1 = 2$ and $w = 0.8$

In this example, γ_2 increases along the dotted straight line starting at $\gamma_1 = 2$ in Figure 3. The monopoly equilibrium is stable for smaller values of γ_2 and loses stability when γ_2 crosses the locus of $L_2(0,0)$ from below. However, it regains stability when γ_2 arrives at the locus of $L_1(0,0)$. When γ_2 is large enough to cross the locus of $L_2(0,1)$ from below, the monopoly equilibrium becomes unstable. This transition of dynamics is illustrated from a different view point as a bifurcation diagram shown in Figure 6(A). The first switching to instability from stability takes place at the left most dotted point, $\gamma_2 \simeq 0.646$.[5] It can be seen that the

[5]This threshold value is calculated as follows. Using the first equation of (2.14) and solving

$$2 = \gamma_1 = \frac{1}{\upsilon}\left(\pi - \sin^{-1}\left[\frac{\upsilon^2 + 2\omega - 1}{2\upsilon\omega}\right] + 2k\pi\right)$$

for υ yields $\upsilon \simeq 0.891$, and then substituting it to the second equation of (2.14) gives $\gamma_2 \simeq 0.646$. Another threshold values are obtained in the same way.

stable equilibrium point bifurcates to a limit cycle having one maximum and one minimum and the amplitude of the cycle gets larger first and then smaller as γ_2 increases. After rapid shrinking of the amplitude, instability switches to stability at the middle dotted point ($\gamma_2 \simeq 5.441$) and thus the trajectory converges to the monopoly equilibrium. At the right most dotted point ($\gamma_2 \simeq 7.697$) a bifurcation to a limit cycle occurs and the expansion phase starts again. Since we set the upper bound of γ_2 to 14 in this example, the equilibrium does not regain stability anymore. We will come back later to the bifurcation cascade defined for $\gamma_2 > 14$ in Example 5 below. As indicated by the shape of the partition curves in Figure 3, the alternation between stability and instability could repeat more frequently for another value of γ_1, especially, for γ_1 closer to γ_1^m. Two limit cycles corresponding to two different values of γ_2 (the blue cycle for $\gamma_2 = 4$ and the red cycle $\gamma_2 = 12$) are illustrated in Figure 6(B).

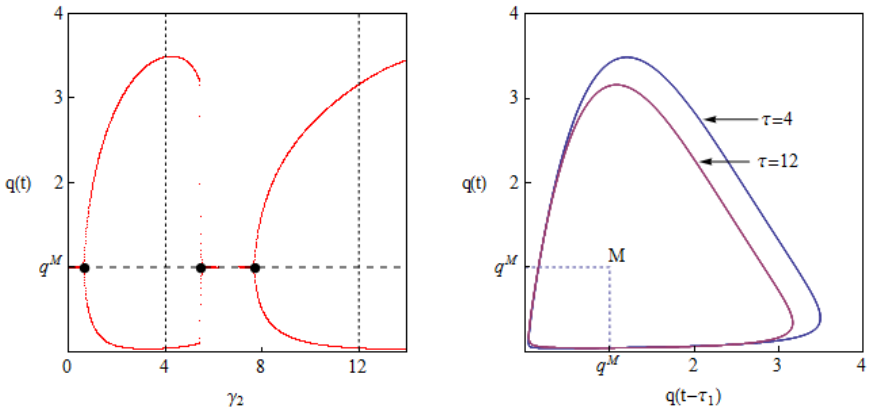

(A) Bifurcation diagram (B) Phase trajectories

Figure 6. Dynamics in Example 1

Example 2: $\gamma_1 = 2.3$ and $w = 0.8$

In this example, γ_1 is taken to be 2.3 and γ_2 is increased from zero up to $7\pi/2(2w-1)(\simeq 18.3)$. As seen in Figure 7(A), limit cycle is born when γ_2 enters into the instability region and its amplitude becomes gradually larger as γ_2 increases. The cycle rapidly becomes smaller when γ_2 approaches the stability-switching point. The equilibrium is stabilized suddenly at the left most dotted point ($\gamma_2 \simeq 6.638$) and destabilized again at the right most dotted point ($\gamma_2 \simeq 8.041$). The bifurcation diagram in the second instability phase implies that the number of trajectory's extrema increases from two to four and then to eight. Further increases of γ_2 then decrease this number from eight to four and finally to two. As a result of increasing γ_1 in this example to 2.3 from the value 2.0 of the previous example, the bifurcation process becomes a little bit complicated and the delay equation generates a multi-period cycle. In Figure 7(B) a four-period cycle is illustrated for $\gamma_2 = 11$.

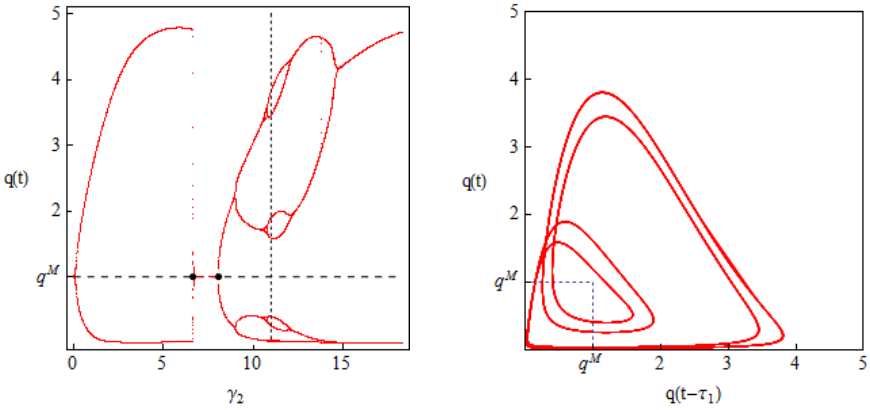

(A) Bifurcation diagram (B) Phase trajectory

Figure 7. Dynamics in Example 2

Example 3: $\gamma_1 = 2.5$ and $w = 0.8$

We increase the value of γ_1 to 2.5 and take the upper bound of γ_2 as $7\pi/(2(2w-1))$ again. It can be seen in Figure 8(A) that the interval of γ_2 can be divided into two instability phases. In the first phase in which γ_2 is less than 7.397, dynamic behavior is almost the same as in the previous examples, although the monopoly equilibrium is now already unstable for $\gamma_2 = 0$. Interesting dynamics appears in the second instability phase in which the monopoly equilibrium undergoes a number-doubling cascade, a chaotic cascade and a number-halving cascade.[6] The birth of complicated dynamics could be due to a larger value of γ_1. Figure 8(B) displays a chaotic process of $q(t-\tau_1)$ and $q(t)$ for $\gamma_2 = 14$.

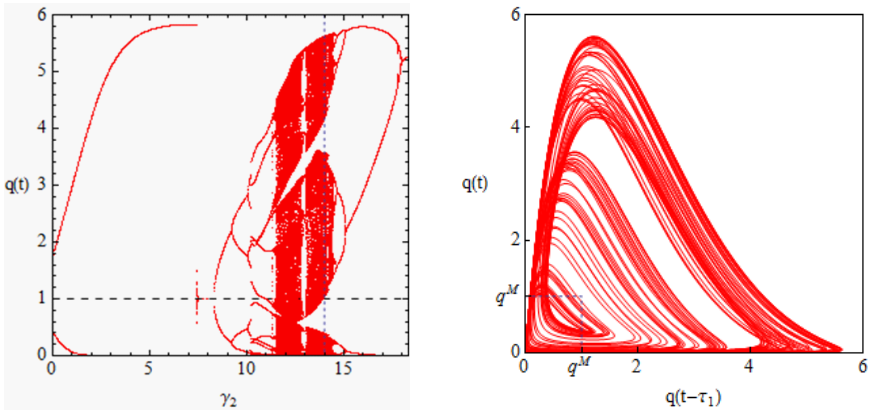

(A) Bifurcation diagram (B) Phase trajectory

Figure 8. Dynamics in Example 3

[6]"number" means the number of the extrema.

Example 4: $\gamma_1 = \frac{\pi}{2} \simeq 1.57$ and $w = 0.5$

In this example we change the value of w to 0.5 and examine dynamics in the case of symmetric weights. Taking $\gamma_1 = \pi/2$, we increase the value of γ_2 from 0 to $9\pi/2$ along the dotted vertical line passing through the points, $(\pi/2, 5\pi/2)$ and $(\pi/2, 9\pi/2)$ in Figure 4. The monopoly equilibrium is locally asymptotically stable for $\gamma_2 \leq \pi/2$. After it loses stability, there is a number-increasing cascade. In Figures 9(B) and (C), we display a one-period cycle with two maxima and two minima and a two-period cycle with three maxima and three minima. As far as the numerical simulations are concerned, only periodic cycles can be born in the symmetric case.

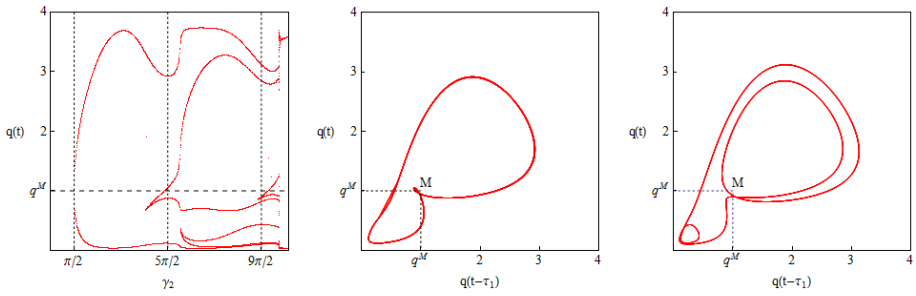

(A) Bifurcation diagram (B) Phase trajectory (C) Phase trajectory

Example 5: $\gamma_1 = 2,\ \omega = 0.8$ and $\gamma_2 > 14$

In the last example, we re-examine dynamics of Example 1 for $\gamma_2 > 14$. Figures 10(A) and (C) are continuations of Figure 5(A) for $\gamma_2 > 14$ and Figure 10(B) combines Figure 10 (A) and Figure 10(C). The only difference between Figures (A) and (C) is the selection of the initial function for $t < 0$, $q_1(t) = 0.1$ in the former and $q_1(t) = 0.8$ in the latter. The bifurcation diagrams are identical for $\gamma_2 < 14.5$, apparently differ for $15 < \tau_2 < 16$ and then become identical again for γ_2 larger than 16. Figure 10 implies the coexistence of attractors.

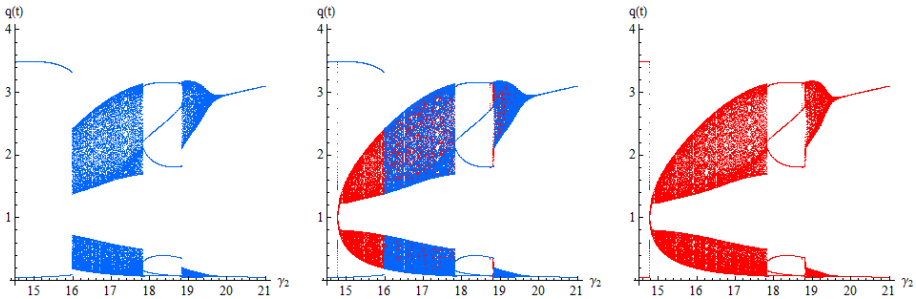

(A) $\phi(t) = 0.1$ (B) Combining (C) $\phi(t) = 0.8$

Figure 10. Dynamics in Example 5

4. Concluding Remarks

This paper constructed a delay monopoly model in which a monopolistic firm was boundedly rational and examined its stability/instability when dynamics was driven by the gradient process. The paper was divided into three parts. In the first part, we assumed that the monopolistic firm had one time delay in its production and detected the threshold value of the production delay at which stability switched to instability. In the second part that was the main part of this paper, we introduced two fixed-time delays into the formation of the expected demand. We first determined the shape of the stability-switch curve that divides the parametric space of the delays into stable and unstable regions. We then showed that the monopoly equilibrium undergoes a Hopf bifurcation when the parameter combination crosses the stability-switch curve. In the final part, we specified parameter values and numerically investigated five special cases in detail in which the global behavior of the equilibrium was illustrated. In particular, it was demonstrated that a one-dimensional differential equation with two fixed-time delays could generate a wide variety of dynamics ranging from a limit cycle to chaos with unstable monopoly equilibrium.

Appendix I

In this Appendix I, we derive relations (2.13) and (2.14) from (2.11) and (2.12). Moving the second term of (2.11) to the right hand side, squaring both sides and using the well-known relation $\cos^2\theta = 1 - \sin^2\theta$ yield

$$\omega^2\left(1-\sin^2(\upsilon\gamma_1)\right) = (1-\omega)^2\left(1-\sin^2(\upsilon\gamma_2)\right).$$

Let $x = \sin(\upsilon\gamma_1)$ and $y = \sin(\upsilon\gamma_2)$. Then the last equation is written as

$$\omega^2(1-x^2) = (1-\omega)^2(1-y^2)$$

which is arranged to be

$$-\omega^2x^2 + (1-\omega)^2y^2 = 1-2\omega. \tag{4.1}$$

Substituting $x = \sin(\upsilon\gamma_1)$ and $y = \sin(\upsilon\gamma_2)$ into equation (2.12) and solving it for y yield

$$y = \frac{\upsilon - \omega x}{1-\omega}. \tag{4.2}$$

Substituting further (4.2) into (4.1) and solving the resultant equation for x give

$$x = \frac{\upsilon^2 + 2\omega - 1}{2\upsilon\omega} \tag{4.3}$$

which is substituted into (4.2) to obtain

$$y = \frac{\upsilon^2 - 2\omega + 1}{2\upsilon(1-\omega)}. \tag{4.4}$$

Replacing x of (4.3) with $\sin(\upsilon\gamma_1)$ and y of (4.4) with $\sin(\upsilon\gamma_2)$, we obtain a parameterized curve in the (γ_1, γ_2) plane:

$$\sin(\upsilon\gamma_1) = \frac{\upsilon^2 + 2\omega - 1}{2\upsilon\omega} \text{ and } \sin(\upsilon\gamma_2) = \frac{\upsilon^2 - 2\omega + 1}{2\upsilon(1-\omega)}. \tag{4.5}$$

In order to have real roots, we need to restrict the range of each of the right hand sides as

$$-1 \le \frac{\upsilon^2 + 2\omega - 1}{2\upsilon\omega} \le 1 \text{ and } -1 \le \frac{\upsilon^2 - 2\omega + 1}{2\upsilon(1-\omega)} \le 1.$$

With $\upsilon > 0$ and $1 > \omega \ge 1/2$, these inequality conditions are reduced to

$$2\omega - 1 \le \upsilon \le 1.$$

Since $\upsilon^2 + 2\omega - 1 > 0$ for $\upsilon \in [2\omega - 1, 1]$, solving the first equation in (4.5) yields infinitely many solutions of γ_1:

$$\gamma_1 = \frac{1}{\upsilon}\left(\sin^{-1}\left[\frac{\upsilon^2 + 2\omega - 1}{2\upsilon\omega}\right] + 2k\pi\right) \text{ with } k \in \mathbb{N} \tag{4.6}$$

or

$$\gamma_1 = \frac{1}{\upsilon}\left(\pi - \sin^{-1}\left[\frac{\upsilon^2 + 2\omega - 1}{2\upsilon\omega}\right] + 2\ell\pi\right) \text{ with } \ell \in \mathbb{N} \tag{4.7}$$

where $\mathbb{N}$ is a set of nonnegative integers.

We next determine γ_2. Since $\upsilon^2 - 2\omega + 1$ can have both signs, we solve the second equation of (4.5) in two cases: $\upsilon \ge \sqrt{2\omega - 1}$ and $\upsilon < \sqrt{2\omega - 1}$. In the first case, $\upsilon^2 - 2\omega + 1$ is nonnegative and thus $\sin(\upsilon\gamma_2) \ge 0$ while in the second case $\upsilon^2 - 2\omega + 1 < 0$ and so $sin(\upsilon\gamma_2) < 0$. Therefore in both cases we have infinitely many solutions of γ_2 in the form

$$\gamma_2 = \frac{1}{\upsilon}\left(\sin^{-1}\left[\frac{\upsilon^2 - 2\omega + 1}{2\upsilon(1-\omega)}\right] + 2m\pi\right) \text{ with } m \in \mathbb{N} \tag{4.8}$$

or

$$\gamma_2 = \frac{1}{\upsilon}\left(\pi - \sin^{-1}\left[\frac{\upsilon^2 - 2\omega + 1}{2\upsilon(1-\omega)}\right] + 2n\pi\right) \text{ with } n \in \mathbb{N}. \tag{4.9}$$

Two solutions of γ_1 and two solutions of γ_2 produce four combinations. However, only two combinations of (γ_1, γ_2) are possible since the sign of $\cos(\upsilon\gamma_2)$ must be different from the sign of $\cos(\upsilon\gamma_1)$ due to (2.11):

if γ_1 is given by (4.6), then γ_2 is given by (4.9)

and

if γ_1 is given by (4.7), then γ_2 is given by (4.8).

Therefore we have two loci of (γ_1, γ_2) for each $k, n \in \mathbb{N}$ given in (2.13) and (2.14).

Appendix II

In this Appendix II, we will analyze the dependence of γ_1 and γ_2 on υ in order to examine the shape of the loci. Consider first a segment $L_1(k, n)$. Simple differentiation shows that

$$\left.\frac{\partial\gamma_1}{\partial\upsilon}\right|_{L_1} = -\tfrac{1}{\upsilon^2}\left(\sin^{-1}\left(\tfrac{\upsilon^2+2\omega-1}{2\upsilon\omega}\right) + 2k\pi\right) + \tfrac{1}{\upsilon}\frac{-1}{\sqrt{1-\left(\frac{\upsilon^2+2\omega-1}{2\upsilon\omega}\right)^2}}\frac{\upsilon^2-2\omega+1}{2\upsilon^2\omega}$$

$$= -\frac{1}{\upsilon^2}\upsilon\gamma_1 + \frac{1}{\upsilon^2\cos(\upsilon\gamma_1)}\sin(\upsilon\gamma_2)\frac{1-\omega}{\omega}$$

We use the first equation of (2.13) and (2.11) to obtain

$$\left.\frac{\partial \gamma_1}{\partial \upsilon}\right|_{L_1} = -\frac{1}{\upsilon^2}\left(\upsilon\gamma_1 + \tan(\upsilon\gamma_2)\right) \tag{4.10}$$

Since $\cos(\upsilon\gamma_1) < 0$ on $L_2(k,n)$, we also have

$$\left.\frac{\partial \gamma_1}{\partial \upsilon}\right|_{L_2} = -\frac{1}{\upsilon^2}\left(\upsilon\gamma_1 + \tan(\upsilon\gamma_2)\right). \tag{4.11}$$

Similarly

$$\begin{aligned}\left.\frac{\partial \gamma_2}{\partial \upsilon}\right|_{L_1} &= -\tfrac{1}{\upsilon^2}\left(\pi - \sin^{-1}\left(\tfrac{\upsilon^2-2\omega+1}{2\upsilon(1-\omega)}\right) + 2n\pi\right) + \tfrac{1}{\upsilon}\frac{-1}{\sqrt{1-\left(\frac{\upsilon^2-2\omega+1}{2\upsilon(1-\omega)}\right)^2}}\tfrac{\upsilon^2+2\omega-1}{2\upsilon(1-\omega)} \\ &= -\frac{1}{\upsilon^2}\upsilon\gamma_2 + \frac{1}{\upsilon^2\cos(\upsilon\gamma_2)}\sin(\upsilon\gamma_1)\frac{\omega}{1-\omega}\end{aligned}$$

Therefore we have

$$\left.\frac{\partial \gamma_2}{\partial \upsilon}\right|_{L_1} = -\frac{1}{\upsilon^2}\left(\upsilon\gamma_2 + \tan(\upsilon\gamma_1)\right) \tag{4.12}$$

and

$$\left.\frac{\partial \gamma_2}{\partial \upsilon}\right|_{L_2} = -\frac{1}{\upsilon^2}\left(\upsilon\gamma_2 + \tan(\upsilon\gamma_1)\right), \tag{4.13}$$

since $\cos(\upsilon\gamma_2) > 0$ on $L_2(k,n)$.

References

[1] Bélair, J. and M. Mackey, "Consumer Memory and Price Fluctuations in Commodity Markets: An Integrodifferential Model," *Journal of Dynamics and Differential Equations,* 1 (1989), 299-325.

[2] Bischi, G. I., C. Chiarella, M. Kopel and F. Szidarovszky, *Nonlinear Oligopolies: Stability and Bifurcations*, 2010, Berlin/Heidelberg/New York, Springer-Verlag.

[3] Bischi, G. I. and F. Lamantia, "Chaos Synchronization and Intermittency in a Duopoly Game with Spillover Effects," in *Oligopoly Dynamics*, T. Puu and I. Sushko (eds), 195-217, 2002, Berlin/Heidelberg/New York, Springer-Verlag.

[4] Bischi, G. I. and A. Naimzada, "Global Analysis of a Duopoly Game with Bounded Rationality," *Advances in Dynamic Games and Applications,* 5 (1999), 361-385.

[5] Chiarella, C. and A. Khomin, "An Analysis of the Complex Dynamic Behavior of Nonlinear Oligopoly Models with Time Lags," *Chaos, Solitons and Fractals,* 7 (1996), 2049-2066.

[6] Chiarella, C. and F. Szidarovszky, "The Birth of Limit Cycles in Nonlinear Oligopolies with Continuously Distributed Information Lags," in *Modeling Uncertainty*, Dror, M., P. L'Ecuyer and F. Szidarovszky (eds), (2001), 249-268, Boston, Kluwer Academic Publisher.

[7] Cooke, K. L. and Z. Grossman, "Discrete Delay, Distributed Delay and Stability Switches," *Journal of Mathematical Analysis and Applications*, 86 (1982), 592-627.

[8] Frich, R. and H. Holme, "The Characteristic Solutions of a Mixed Difference and Differential Equation Occuring in Economic Dynamics," Econometrica, 3 (1935), 225-239.

[9] Hale, J., "Nonlinear Oscillations in Equations with Delays," in *Nonlinear Oscillations in Biology (Lectures in Applied Mathematics, 17)*, Hoppenstadt K. C. (ed), (1979), 157-185, American Mathematical Society.

[10] Hale, J. and W. Huang, "Global Geometry of the Stable Regions for Two Delay Differential Equations," *Journal of Mathematical Analysis and Applications*, 178 (1993), 344-362.

[11] Howroyd, T. and A. Russel, "Cournot Oligopoly Models with Time Delays," *Journal of Mathematical Economics*, 13 (1984), 97-103.

[12] Invernizzi, S. and A. Medio, "On Lags and Chaos in Economic Dynamic Models," *Journal of Mathematical Economics*, 20 (1991), 521-550.

[13] Matsumoto, A., "Note on Goodwin's 1951 Nonlinear Accelerator Model with an Investment Lag," *Journal of Economic Dynamics and Control*, 33 (2009), 832-842.

[14] Matsumoto, A. and F. Szidarovszky, "Delay Differential Neoclassical Growth Model," *Journal of Economic Behavior and Organization,* 78 (2011a), 272-289.

[15] Matsumoto, A. and F. Szidarovszky, "An Elementary Study of a Class of Dynamic Systems with Single Time Delay," DP 161 (http://www2.chuo-u.ac.jp/keizaiken/discuss.htm), Institute of Economic Research, Chuo University, 2011b.

[16] Matsumoto, A. and F. Szidarovszky, "An Elementary Study of a Class of Dynamic Systems with Two Time Delays," DP 162 (http://www2.chuo-u.ac.jp/keizaiken/discuss.htm), Institute of Economic Research, Chuo University, 2011c.

[17] Naimzada, A., "A Delay Economic Model with Flexible Time Lag," *mimeo*, 2011.

[18] Puu, T. *Attractors, Bifurcations and Chaos*, 2003, Berlin/Heidelberg/New York, Springer-Verlag.

[19] Wright, E. M. "On a Class of Prey-Predator Population Models with Time Lag," *Acta Mathematica Applicatae Sinica*, 11 (1955), 12-21.

Current address: Akio Matsumoto: Department of Economics, Chuo University, 742-1, Higashi-Nakano, Hachioji, Tokyo, 192-0393, Japan.

E-mail address: akiom@tamacc.chuo-u.ac.jp

Current address: Ferenc Szidarovzky: Department of Systems and Industrial Engineering, University of Arizona, Tucson, Arizona, 85721-0020, USA.

E-mail address: szidar@sie.arizona.edu